

# PROSTATE SEGMENTATION IN ECHOGRAPHIC IMAGES: A VARIATIONAL APPROACH USING DEFORMABLE SUPER-ELLIPSE AND RAYLEIGH DISTRIBUTION

*Laurent Saroul, Olivier Bernard, Didier Vray, Denis Friboulet*

CREATIS-LRMN, CNRS UMR 5220, INSERM U630,  
INSA-Lyon, F-69621 Villeurbanne, France

## ABSTRACT

We present a simple, robust and computationally efficient method for the semi-automatic segmentation of the prostate in TRUS (Transrectal Ultrasound) image. The method relies on a variational formulation based on a deformable super-ellipse and a region energy based on the assumption of a Rayleigh distribution. Instead of using the classical level-set approach, we directly insert the implicit representation of a deformable super-ellipse into the energy to minimize. This yields a super-ellipse evolution able to accurately segment prostate and surrounding tissues while handling boundary gaps on the contour.

**Index Terms** — Prostate, Echography, Segmentation, Variational active contours, Rayleigh distribution, Deformable super-ellipse.

## 1. INTRODUCTION

Automatic segmentation of prostate in TRUS image has been the subject of great research effort during the last past years. The main difficulties which arise when processing TRUS images of the prostate are the poor contrast between the prostate and the surrounding tissues, the non-homogenous texture of the prostate together with speckle noise, missing boundaries due to acoustic shadowing and boundaries parallel to the ultrasound beam (see Figs. 2, 4 and 5).

As a consequence, classical segmentation techniques using gradient information fail when used directly on these images. Several pre-processing steps are then required, in order to remove the speckle noise and increase contrast between the different regions [1,2]. In order to handle boundary gaps in the contour, several authors proposed to introduce a shape prior, allowing thereby constraining the geometry of the resulting contour [3]. For that purpose, statistical mean shape built from a large database of manually delineated prostate contours was introduced. An example of such approach is described in [4], where an active shape model coupled with Gabor texture filter was successfully applied to the 2D and 3D segmentation of the prostate.

In [5], the authors show that the prostate boundary may be successfully approximated by a super-ellipse with additional global deformation terms such as tapering and bending. Since the super-ellipse is deformed through gradient information, the initial contour needs to be placed close to the contour of the prostate. Therefore, they propose a Bayesian approach which also uses statistics on the pose and shape of the contour.

In contrast with this last method, we propose in this paper a variational approach where the active contour is modelled through the implicit representation of a super-ellipse. We minimize a region energy based on the assumption of a Rayleigh distribution of the intensities within the image. This approach has the following potential advantages over the previous works:

- The shape prior is simple and do not imply the manual processing of large amount of data needed to build mean shape, which is moreover orientation dependant.
- The use of region terms based on image statistical features is more robust than gradient information for US images and avoids the use of heavy pre-processing steps [1,3,5].

Note that a similar idea has been suggested by [6] in the field of echocardiography where a simple ellipse is used as the shape constraint. Our approach is more general since we propose a more flexible shape a priori through a super-ellipse with tapering.

We present in section 2 the theoretical formulation of the super-ellipse evolution. We give in section 3 the details of the application of the approach to TRUS prostate images. We finally present the obtained experimental results in section 4.

## 2. THEORETICAL FORMULATION

### 2.1 Choice of the shape model

Since the acquisition is made with a sectorial probe, the raw US data are given in polar geometry. We decide to work directly with this representation, since the shape of the prostate is fairly simple when using this geometry (see Fig. 4) and can be accurately modelled by a deformable

super-ellipse, without the additional bending term used in [5]. Moreover, working directly on such data removes the need for data interpolation which may induce artefacts since our approach is based on statistics.

## 2.2 Super-Ellipse formulation

A point  $P(x, y)$  belonging to a super-ellipse with main axes aligned with the coordinate axes verifies the following implicit equation:

$$S(P) = \left(\frac{x^2}{a^2}\right)^{\frac{1}{\varepsilon_1}} + \left(\frac{y^2}{b^2}\right)^{\frac{1}{\varepsilon_1}} - 1 = 0 \quad (1)$$

where  $\varepsilon_1$  is the squareness and  $(a, b)$  the semi-axes length of the super-ellipse.

This equation can be made more general by allowing rotation, translation and linear tapering along  $y$  axis. The linear tapering is defined by the following transform:

$$(x', y') = \left( \left(\frac{ty}{b} + 1\right)x, y \right) \quad (2)$$

where  $t \in [-1, 1]$  is the tapering parameter.

Let us define  $Tr$  as the translation of vector  $(x_c, y_c)$ ,  $R$  as the rotation of angle  $\theta$ , and  $Tp$  the tapering of parameter  $t$ . The equation of the deformed super-ellipse is then given as:

$$S_\Gamma(P) = S(F_\Gamma^{-1}(P)) = 0 \quad (3)$$

Where  $F_\Gamma = Tr \circ R \circ Tp$  and

$$\Gamma = \{v_k\}_{1 \leq k \leq 7} = [x_c, y_c, \theta, a, b, \varepsilon_1, t], \quad (4)$$

is the set of parameters defining the super-ellipse.

## 2.3. Super-ellipse evolution

We consider the following general energy to minimize [7]:

$$E = \iint_{\Omega_{in}} g_{in}(I(\mathbf{x}))d\mathbf{x} + \iint_{\Omega_{out}} g_{out}(I(\mathbf{x}))d\mathbf{x} \quad (5)$$

where  $g$  is a region term reflecting the image features characterizing the object to be segmented. In conventional approaches, this energy can be minimized using level-set methods [7,8].

In contrast with these classical approaches, we constrain the solution to be a super-ellipse by incorporating the implicit function  $S_\Gamma$  into (5), which yields:

$$E = \iint_{\Omega} [g_{out}(I(\mathbf{x}))H_\varepsilon(S_\Gamma(\mathbf{x})) + g_{in}(I(\mathbf{x}))(1 - H_\varepsilon(S_\Gamma(\mathbf{x})))d\mathbf{x} \quad (6)$$

where  $H_\varepsilon(\cdot)$  is a regularized Heaviside function [7]. In order to reach a local minimum of the energy (5) according

to the seven parameters defining the super-ellipse, we use a gradient-descent method which yields:

$$v_k^{(n+1)} = v_k^{(n)} - \lambda_k \frac{\partial E(\Gamma^{(n)})}{\partial v_k} \quad (7)$$

The derivatives of the energy are given as:

$$\frac{\partial E}{\partial v_k} = \iint_{\Omega} [g_{out}(I(\mathbf{x})) - g_{in}(I(\mathbf{x}))] \delta_\varepsilon(S_\Gamma(\mathbf{x})) \frac{\partial S_\Gamma(\mathbf{x})}{\partial v_k} d\mathbf{x} \quad (8)$$

where  $\delta_\varepsilon(\cdot)$  is a regularized Dirac function [7].

Thanks to their analytic form, the derivatives of  $S_\Gamma$  according to  $\{v_k\}$  may be easily computed. We use different time steps  $\{\lambda_k\}$  since the super-ellipse parameters have not the same geometric meaning and the same range of values.

## 2.4 Statistical region term

In order to take into account the distribution of the intensities into the energy to minimize, we look for the curve that maximizes the likelihood function given by the product of the inner and the outer probability [8,9,10]. This leads to minimize the following energy:

$$E = \iint_{\Omega_{in}} -\log p_{in}(I(\mathbf{x}))d\mathbf{x} + \iint_{\Omega_{out}} -\log p_{out}(I(\mathbf{x}))d\mathbf{x} \quad (9)$$

where  $p_{in}(I)$  and  $p_{out}(I)$  are, respectively, the probability of the intensity  $I$  to belong to, resp.,  $\Omega_{in}$  and  $\Omega_{out}$ . With this formulation, more sophisticated assumptions on the statistical distribution of the intensity in  $\Omega_{in}$  and  $\Omega_{out}$  may be introduced.

## 2.5. Numerical Implementation

In order to reach the local minimum of (9), we use a conventional Expectation Minimization Technique. First, considering  $S_\Gamma$  fixed (i.e.  $\{v_k\}$  fixed), we estimate the distribution parameters in  $\Omega_{in}$  and  $\Omega_{out}$  (see Section 3). Then, by considering  $\log p(I)$  fixed for all pixels  $(i, j)$  in  $\Omega$ , we minimize (9) according to  $\{v_k\}$  by using (7). The equation (7) is discretized as:

$$v_k^{(n+1)} = v_k^{(n)} - \lambda_k \sum_{i,j} \log \frac{p_{out}^{(n)}(i,j)}{p_{in}^{(n)}(i,j)} \cdot \delta_\varepsilon(S_{\Gamma^{(n)}}(i,j)) \cdot \frac{\partial S_{\Gamma^{(n)}}(i,j)}{\partial v_k} \quad (10)$$

The two above steps are repeated until convergence of the parameters. Fig. 1 shows an example of the method on a simulated image representing a super-ellipse with additive Gaussian noise (SNR = 20 dB) and a simulated acoustic shadow. For that example, we use a Gaussian distribution of intensities. The initial contour is a small circle (Fig. 1a). The convergence is reached in 70 iterations, and the final super-ellipse parameters found by the algorithm are close to the

theoretical ones. This example shows that, by using the super-ellipse shape constraint, the algorithm is able to segment partially occluded object.

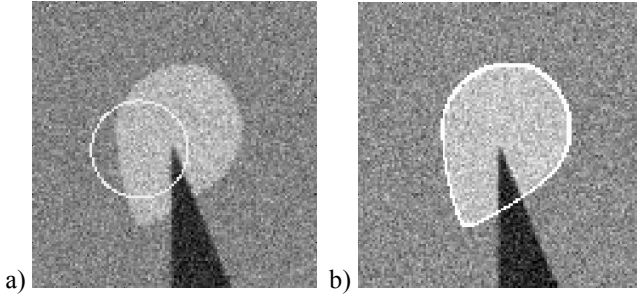


Figure 1. Segmentation of a simulated image (120 x 120 pixels) using our approach

### 3. APPLICATION TO PROSTATE ECHOGRAPHIC POLAR IMAGES

#### 3.1. Image statistics

The a priori distribution for image intensities is chosen to be the Rayleigh distribution, which is a classical statistical model for the envelope signal (without logarithmic compression) in the case of fully developed speckle [8], i.e.

$p(I) = \frac{I}{\sigma^2} \exp\left(-\frac{I^2}{2\sigma^2}\right)$ . The Rayleigh distribution parameter  $\sigma$  is computed using its maximum likelihood expression [8]:  $\hat{\sigma}^2 = \frac{\sum I^2}{2N}$ , where  $N$  is the number of

samples. Fig. 2 shows that this distribution is able to accurately fit the empirical distributions of intensities within the different regions of the prostate.

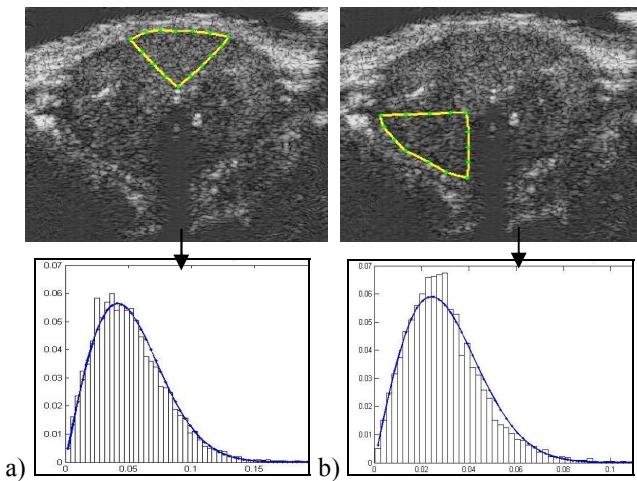


Figure 2. Experimental intensity distribution and Rayleigh distribution fitting within different parts of the prostate

#### 3.2. Partitioning the image domain

Due to attenuation and to the inhomogeneous structure of the tissue, the parameters of the Rayleigh distribution depends on the location within the prostate. Fig. 2 illustrates this phenomenon on two regions where the parameter  $\sigma$  is 0.0017 (Fig. 2a) and 0.00058 (Fig. 2b).

We propose to take this non-stationarity into account by letting the distribution parameters vary along the orthoradial direction according to the center of the super-ellipse. This results in replacing  $p(I)$  by  $p_{\varphi_i}(I)$  in (9), where  $\varphi_i$  represents an angular sector of the image according to the center of the ellipse. The parameter  $\sigma_{\varphi_i}$  of  $p_{\varphi_i}$  is estimated by only considering pixels included in  $\varphi_i$ .

The choice of the angular partitioning yields the usual trade-off between resolution and variance in the estimation of the distribution parameters. Indeed, small sectors ensure high spatial resolution but in turns yield a high variance of the estimations. We choose in the present implementation to partition the whole domain into eight angular sectors according to the current super-ellipse center, as shown in Fig. 3. The optimality of this choice is difficult to assert, however experimental results show that such partition yields satisfying segmentations and that increasing the number of sectors does not bring any improvement.

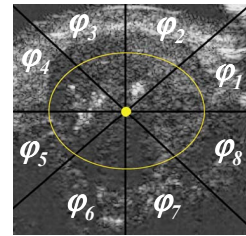


Figure 3. Angular partition for prostate images

### 4. RESULTS AND EXPERIMENTS

The initial contour is selected as circle centered on the prostate (Fig. 4, dot circles). The time-steps  $\{\lambda_k\}$  are initialized to 1 for  $[x_c, y_c, a, b]$  and to 0.005 for  $[\theta, \varepsilon_1, t]$ . The parameter of the regularized Dirac function is set to 0.1. These parameters were kept constant for all experiments.

We test our algorithm on several TRUS images. Examples of segmentation in the initial polar coordinates are shown in Fig. 4. Four examples of resulting segmentation in Cartesian coordinates are shown in Fig. 5.

Thanks to the super-ellipse constraint, the algorithm is able to segment the prostate boundary despite of the acoustic shadow in the bottom of the prostate. These examples also demonstrate that by performing the segmentation directly on the polar images, additional deformation of the super-ellipse such as bending is not necessary (Fig. 4).

Moreover, the partition of the prostate into several angular sectors allows to handle the large differences in the intensity distribution within the different parts of the prostate and therefore to accurately separate the prostate and the surrounding tissues.

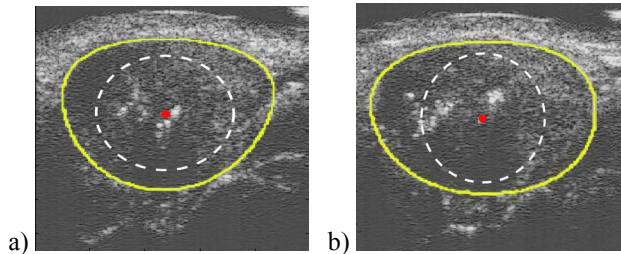


Figure 4. Examples of prostate segmentation on two prostate polar images

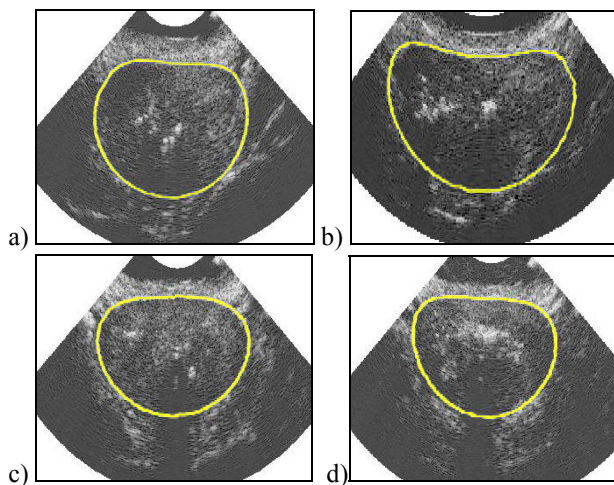


Figure 5. Examples of prostate segmentation on four prostate Cartesian images (performed in 78, 75, 45, and 61 iterations)

## 5. CONCLUSIONS AND PERSPECTIVES

We proposed a new approach for prostate segmentation in TRUS image, using a variational formulation based on a deformable super-ellipse and a region energy based on the assumption of a Rayleigh distribution. The preliminary results show that the shape constraint allows the algorithm to handle the main difficulties in prostate images, in particular large gaps in the boundary induced by acoustic shadowing. The interest of the approach relies on the fact that it avoids the pre-processing steps associated to gradient-based methods and that it does not need statistical mean shape for constraining the algorithm.

The preliminary obtained results are very promising but a larger clinical evaluation will be necessary to validate the robustness of the approach. Moreover, several improvements may be introduced in the algorithm. One future improvement may be the introduction of more

sophisticated distributions, better adapted to the different distributions within the prostate. Finally, we plan to extend the algorithm from 2D to 3D by using super-ellipsoids.

## 6. ACKNOWLEDGMENTS

This work was supported by the French National Research Agency (ANR) through Carnot funding. The TRUS prostate images were provided by INSERM U 556, Laboratory of Therapeutic Applications of Ultrasound.

## 7. REFERENCES

- [1] Pathak, S. D., Chalana, V., Haynor, D. R., and Kim, Y., "Edge-guided boundary delineation in prostate ultrasound images," *IEEE Transaction on Medical Imaging*, 2000, Vol. 19, pp. 1211–1219.
- [2] Ladak, H., Fei, M., Wang, Y., Downey, D., Steinman, D. and Fenster, A., "Prostate segmentation from 2D ultrasound images," in *Proceedings of the International Conference of Engineering in Medicine and Biology Society*, 2000, Vol. 4, pp. 3188-3191.
- [3] Noble, J.A., Boukerroui, D., "Ultrasound image segmentation: a survey," in *IEEE Transactions on Medical Imaging*, 2006, Vol. 25, N°8, pp. 987-1010.
- [4] Hodge, A. C., Fenster, A., Downey, D. B. and Ladak, H. M., "Prostate boundary segmentation from ultrasound images using 2D active shape models: Optimisation and extension to 3D," in *Journal of Computer Methods and Programs in Biomedicine*, 2006, Vol. 84, N° 2, pp. 99-113.
- [5] Gong, L.P., Pathak, S.D., Haynor, D.R., Cho, P.S. and Kim, Y., "Parametric shape modeling using deformable super-ellipses for prostate segmentation," in *IEEE Transactions on Medical Imaging*, 2004, Vol. 23, N°3, pp. 340-349.
- [6] Taron, M., Paragios, N. and Jolly, M.P., "Border detection on short axis echocardiographic views using a region based ellipse-driven framework," in *Proceedings of MICCAI 2004*, Springer-Verlag, Vol. 3216, pp. 443-450.
- [7] Chan, T., Vese, L., "Active contours without edges," in *IEEE Transactions on Image Processing*, 2001, Vol. 10, pp. 266–277.
- [8] Sarti, A.C., Mazzini, E. and Lamberti, C., "Maximum likelihood segmentation of ultrasound images with Rayleigh distribution," in *IEEE Transactions on Ultrasonics, Ferroelectrics and Frequency Control*, 2005, Vol. 52, N°6, pp. 947-960.
- [9] Zhu, S., Yuille, A., "Region competition: Unifying snakes, region growing, and bayes/mdl for multiband image segmentation," in *IEEE Transaction on Pattern Analysis and Machine Intelligence*, 1996, Vol. 18, pp. 884–900.
- [10] Bernard, O., Touil, B., Gelas, A., Prost, R., and Friboulet, D., "Segmentation of myocardial regions in echocardiography using the statistics of the radio-frequency signal" in *Proceedings of Functional Imaging and Modeling of the Heart (FIMH'07)*, 2007, pp. 433-442.